International Journal of Current Engineering and Technology
E-ISSN 2277 – 4106, P-ISSN 2347 – 5161

Available at http://inpressco.com/category/ijcet

Research Article

Recycling Waste Cans to Nano Gamma Alumina: Effect of the Calcination Temperature and pH

Nada Sadoon Ahmedzeki[#*], SattarJalil Hussein[!], Waqar Abdulwahid Abdulnabi[#]

[#]Chemical Engineering Department, College of Engineering, University of Baghdad, Iraq
[!]Petroleum Research and Development Center, Ministry of Oil-Baghdad, Iraq

Accepted 10 Jan 2017, Available online 21 Jan 2017, **Vol.7, No.1 (Feb 2017)**

Abstract

In the present study, the precipitation of aluminum oxide gel from sodium aluminate solution, extracted from the cans, using hydrochloric acid was studied at different pH values of 3, 7, and 12. The effect of the product calcination was also studied at different calcination temperatures. X-ray diffraction (XRD), N_2 adsorption/ desorption isotherms, X-ray fluorescence (XRF) and atomic force microscopy (AFM) were used in the investigation and distinguish between the samples. The results showed that the nano crystalline gamma alumina with an average particle size of 68.56 nm, having high surface area of 311m^2/g, can be obtained by a facile cost effective process.

Keywords: *Waste cans; gamma alumina, calcination; characterization*

Introduction

Alumina has an important industrial applications due to the pronounced physical and chemical properties (Sheel *et al*, 2016; Chotisuwan *et al*, 2012). Refineries are familiar with the gamma phase due to its important use as catalyst support in the hydrotreating processes because of its large surface area, highly porous and excellent mechanical strength (Asenciosa & Sun-Koub 2012). It is also used as a good adsorbent in many processes of drying, sweetening and filtration operations having high industrial potential (Fernando & Chung 2001). Materials with these characteristics have predominate industrial focus offering a long life when used as catalysts and adsorbents (Keshavarz *et al*, 2010).

Aluminum oxide exists in many forms which are produced through the calcination of aluminum hydrates bayerite, gibbsite and boehmite at temperatures ranging between 230-1100ºC (Zhang & Pinnavaia 2008). In this thermal treatment, dehydration causes a series of decompositions and transformations producing different types of aluminum oxides starting from Al(OH)3 , to α-Al2O3(Matori *et al*, 2012). γ-Al2O3is very important among other phases because of its structure possesses high surface which gains the focus for many chemical and petrochemical separation processes and catalysis (Hosseini *et al*, 2011; Bell *et al*, 2015). Also it is used as a ceramic raw material and as gas sensor (An *et al*, 2010).

*Corresponding author: **Nada Sadoon Ahmedzeki**

Investigations for the synthesis of materials by the recycling of wastes are having the interest of many researchers because it solves important environmental problem(s), cost effective from an economic point of view, in addition to its utilization in many potential applications. The aforementioned descriptions reflect the necessary aspects of green technologies.

Liu *et al*, (2011)studied the method for the preparation of micro alpha alumina from beverage aluminum cans by reacting with ethanol and calcinations the product at 900 ºC for 2 h (Liu *et al*, 2011). They suggested the use of vacuum distillation to purify the product due to the presence of some impure oxides.γ-Al2O3was prepared by the reaction of sodium aluminate solution from aluminum scrap and sodium hydroxide and then reacted with sulfuric acid. It was concluded that high surface area (371 m^2/g) could be produced at low pH values and calcination at 500 ºC(Asenciosa & Sun-Koub 2012).

Aluminum isopropoxide and aluminum hydroxide from waste aluminum cans was converted to alumina having high surface area of (421-556 m^2/g) (Chotisuwan *et al*, 2012)at calcinations temperature of 500ºC. Sheel *et al*, (2016) investigated the preparation of aluminum oxide calcined at 800°C from industrial cans by acid and alkali method (Sheel *et al*, 2016). They showed that reacting the cans directly with acid (HCl and NH_4Cl) is more convenient and preferred to prepare alumina than the alkali method (NaOH addition and water) because of its higher product quality and quantity. Also, Aluminum waste dissolution was studied by several researchers using different resources like; KOH addition (Chotisuwan *et al*, 2012),

directH_2SO_4 addition (Dash *et al*, 2008; Das *et al*, 2007) and water addition (Zou *et al*, 2013) where the latter study focused on the hydrogen evolution during the reaction. Martínez *et al*, (2007) reported that 4110Wh can be produced per one kg of Al which is quite interesting for utilization in fuel cells (Martínez *et al*, 2007).

The aim of this work is to investigate the factors affecting the formation of the gamma phase alumina catalyst. No past study of the proposed route in the present work of the recycling of cans. An extensive investigation was employed to specify the pH of the reaction in the acid addition step and the best calcination temperature of the product. The sodium aluminate solution obtained from the reaction of aluminum cans and sodium hydroxide was treated with hydrochloric acid. Samples of the prepared alumina were characterized and distinguished by their XRD patterns, % crystallinity, crystallite size and surface area to find out the best quality of the catalyst.

Experimental

Waste cans were reacted with 40% sodium hydroxide solution. After solid separation, the pH value of the sodium aluminate solution was adjusted using concentrated hydrochloric acid to 3, 7 and 12. This solution was aged for 6 hat 80º C. Aluminum hydroxide gel was washed with deionized water, filtered and dried at 80º C for 6 h. Calcination was at 550, 600 and 650 ^{o}C for 3 h in air at a heating rate of 1º C/min.

Results and Discussion

Catalyst Characterization

Effect of Calcination Temperatures on XRD

The calcination temperature is considered as the most important factor that affecting alumina structure because it controls the dehydration process of aluminum hydroxides precipitations which lead to produce alumina with different properties for several applications (Amirsalari & Farjami Shayesteh 2015). In order to study this effect, the calcinations of aluminum hydroxides precipitated at pH 3 were investigated at 550, 600 and 650ºC, and the XRD patterns were shown in figures 1, 2 and 3 respectively.

As shown in figure 1, the XRD peaks can be assigned to gamma alumina structure characterized by 2θ at 66.87, 45.85 with broad peak at 37.42ºrespectively. It can be seen that these peaks tends to be amorphous due to their low intensities(Du *et al*, 2009). It was obvious from figure 2 that increasing calcinations temperature to 600ºC showed a comparable pattern with the characteristic peaks located at 2θ of 66.97, 45.91 and 37.48º.

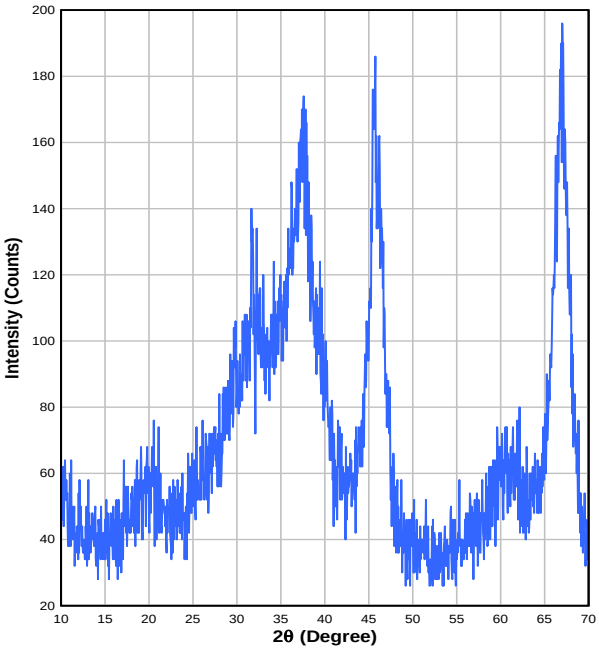

Fig.1 XRD pattern of alumina calcined at 550 ºC

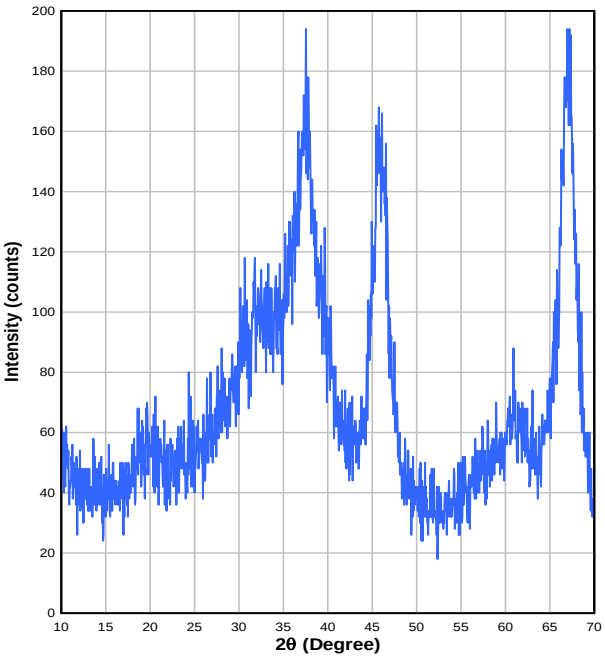

Fig.2 XRD pattern of alumina calcined at 600 ºC

Alumina remained in an amorphous structure even after increasing the calcinations temperature to 650 ºC and the intensities of the visible peaks became stronger as shown in figure 3. These peaks were also corresponded to gamma alumina major diffraction peaks at 2θ of 66.907, 45.88 and 37.46 º respectively. It is noticeable that alumina calcined at 550, 600 and 650 ºC had identical XRD peaks positions. This may be due to the unit cell symmetry (Amirsalari & Farjami Shayesteh 2015). In the present study, highly crystalline material is produced by increasing calcination temperatures due to increasing the intensities of the diffraction peaks, which is in turn

indicates the increase of the crystals growth (Hummadi 2005).

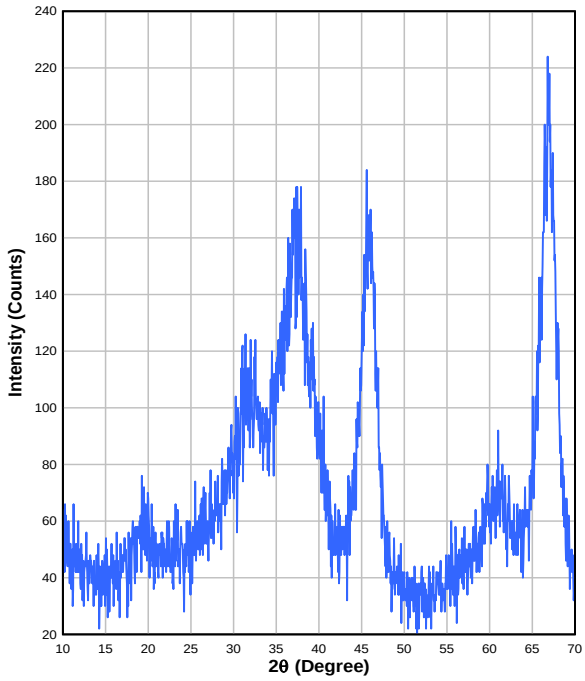

Fig.3 XRD pattern of alumina calcined at 650 ºC

According to figures 1 to3, a calcination temperature of 550 ºC showed splitting peak located at 2θ of 31.8º. Increasing the calcinations temperature to 650 ºC, decreased the degree of splitting of peaks found at 2θ of 31.75º due to the decrease of tetragonal distortion. In other words, peaks asymmetry or splitting indicates a tetragonal structure of γ -Al_2O_3 phase as was cited by(Amirsalari & Farjami Shayesteh 2015). As reported in the past studies, generally γ -Al_2O_3phase is cubic and a tetragonal distortion of cubic lattice can occur during the converting boehmite to γ -Al_2O_3 (Yamaguchi *et al*, 1964; Sickafus *et al*, 1999; De Boer & Lippens 1964).The presence of a dual-phase(cubic and tetragonal) γ -$Al_2O_3$was confirmed by many researchers. The tetragonal system is found at low temperature and the cubic γ -Al_2O_3in high temperature at the expense of tetragonal(Amirsalari & Farjami Shayesteh 2015).

The degree of relative crystallinity of alumina calcined at different temperatures was investigated as shown in figure 4. The crystallinity of the samples was determined according to equation 1 (Al-rubaye 2013).

$$Average\ Crystallinity\ \% = \frac{\sum Intensities\ of\ peak\ of\ sample}{\sum Intensities\ of\ peaks\ of\ reference\ sample} \times 100 \qquad (1)$$

According to figure 4, it was clear that the relative crystallinity increased from 91.4 to 96.7% as the calcination temperature increased from 550 to 600˚ C, it would then slightly decreased to 96.33 % as the temperature increased to 650˚ C. This behavior indicates that as the calcination temperature increased, the crystallization degree increased and it would slow down with further increasing in temperature. This is in agreement with Monshi who reported that the nano crystallite growth was highly promoted at the lower temperatures, but it would less affected at higher temperatures (Monshi *et al*, 2012).

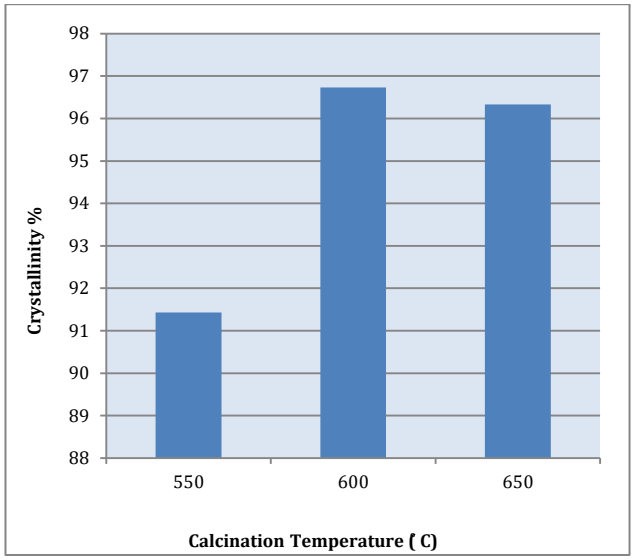

Fig.4 Average crystallinity versus calcination temperature

In order to examine the effect of calcination temperature on the size of crystallite, alumina crystalline sizes were calculated from the major diffraction peaks using Scherrer's equation (2) (Monshi *et al*, 2012):

$$d = \frac{0.94\lambda}{\beta cos\theta} \qquad (2)$$

where d is the size of crystallite, λ is the X-ray wavelength in nanometer (nm), β represents the full width at half maximum (FWHM) in radiant and θ is the Bragg angle. The calculated crystalline sizes of alumina calcined at 550, 600 and 650 ºC are listed in tables 1, 2 and 3 respectively.

Table 1 XRD data of alumina calcined at 550 ºC

2θ	I/Iº	FWHM	d (nm)
66.870	100	1.970	5.044
45.850	76	1.840	4.895
37.423	48	2.375	3.688
			Ave. 4.542

Table 2 XRD data of alumina calcined at 600 ºC

2θ	I/Iº	FWHM	d (nm)
66.978	100	1.787	5.565
45.917	80	1.875	4.805
37.485	57	1.800	4.867
			Ave. 5.079

Table 3 XRD data of alumina calcined at 650 ºC

2θ	I/Iº	FWHM	d (nm)
66.907	100	1.830	5.433
45.886	85	1.787	5.039
37.460	51	1.850	4.735
			Ave. 5.069

As listed in tables 1 to 3, when the calcination temperatures increased from 550 to 600 ºC the crystallites size increased from 4.542 to 5.079 nm, the size of the crystallites decreased only slightly to 5.069 nm at 650 ºC. It is well known that the crystallite size increases linearly with increasing calcination temperature until a constant size is achieved. The increasing in crystallite size can be attributed to the promoted crystallite growth during the calcination process because of a tendency for minimization of the interfacial surface energy (Monshi *et al*, 2012; Chen *et al*, 2003).According to the finding observed by (Asenciosa & Sun-Koub 2012), nucleation process was accelerated at high temperatures where aluminum hydroxide particles were solubilized and grew during condensation reactions; particles with larger sizes will be formed through this growth.

Effect of Calcination Temperature on surface area

The relationship between calcination temperature, surface area and crystallite sizes of samples were illustrated in table 4, it was clear that the surface area decreased by increasing calcinations temperature and a maximum surface area of 279.11m²/g was obtained at calcination temperature of 550 ºC, while the crystallite sizes showed an increasing trend from 4.542 to 5.069 nm with increasing the calcination temperature from 550 to 650 ºC. The decrease in surface area as a result of increasing calcinations temperatures may be due to the increase in crystallite sizes. This is in agreement with the findings reported earlier (Gaber *et al*, 2014; Taies & Mahmood 2010).

Table 4 Surface area and crystallite size and calcination temperatures

Temperature	Surface Area	Crystallite Size
(ºC)	(m²/g)	(nm)
550	279.11	4.542
600	253.67	5.079
650	246.14	5.069

As reported in other studies (Chen *et al*, 2003; Richardson 1989), maximum surface areas were obtained from smaller crystallite sizes. These crystallites contained high proportion of small pores. Increasing calcinations temperatures led to the increase in the rate of evaporation of water and gases (OH bond and CO gas) entrapped in the small pores towards larger ones and then to the bulk causing a drop in pressure. This pressure drop would be resulted in a partial loss of surface area due to the collapse of part of the pores.

Wang *et al*, (2008) concluded that the calcination temperature was the important factor in the surface area study. The reaction is accelerated at higher calcination temperatures and as a result increases the contact of crystallites between each other. So that at higher temperatures smaller crystallites will be coalesced and form crystallite with larger size. This coalescing step will decrease pore volume and surface area of the sample by crystallite sintering or agglomeration phenomena (Richardson 1989; Gaber *et al*, 2014). Therefore, the calcination temperature of 550 ºC was chosen for further pH study.

Effect of pH of Reaction on XRD

The pH of the solution is an important parameter that strongly affects the solution reaction and phase transformation of alumina produced from the calcinations of aluminum hydroxide precipitated at this pH condition (Asenciosa & Sun-Koub 2012). In order to study this effect, the solution pH was varied over a range of 3 to 12. Samples were characterized by X-Ray diffraction (XRD) as shown in figures 1, 5 and 6.

As was discussed, figure 1 showed the XRD pattern of the sample which was adjusted to pH value of 3 and the resulting diffraction peaks confirmed the formation of gamma alumina by hydrothermal treatment of aluminum hydroxide precipitated at this pH value. By increasing pH conditions to 7, the diffraction peaks were also attributed to gamma alumina structure at 2θ of 66.57, 45.88 and 37.18º. However figure 5 showed a slight shift in the positions of the recognized peaks and their intensities when compared with the standard peaks which may be due to the non-stoichiometry of the composition and waste heterogeneity (Liu *et al*, 2011).

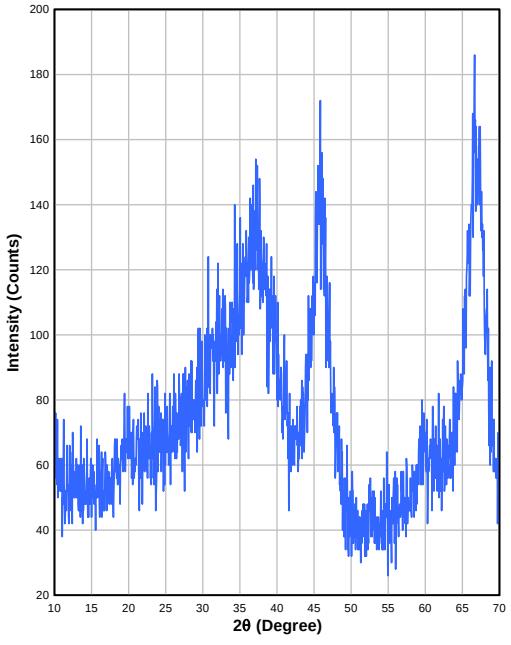

Fig 5 XRD pattern of alumina synthesized at pH 7

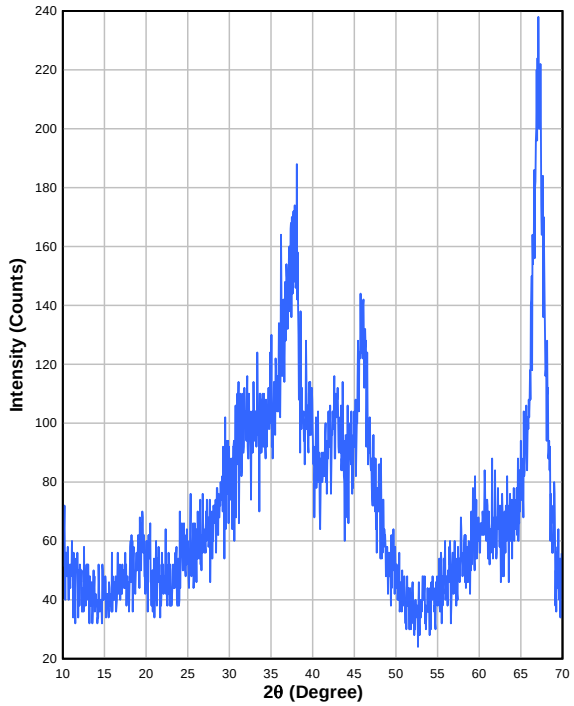

Fig 6 XRD pattern of alumina synthesized at pH 12

Further increase in pH value to 12, a single gamma alumina phase was also recognized by its characteristics diffraction peaks at 2θ values of 67.07, 46.01 and 37.51º respectively as shown in figure 6.

From the observed XRD patterns, a characteristic of nano sized an amorphous structure was recognized due to the broadening and low intensities of the corresponding peaks (Sun *et al*, 2008; Yaripour *et al*, 2015).

As can be seen from figures 4.5, 4.9 and 4.10, the intensities of the diffraction peaks increased with increasing pH of the solution. The same results can be found in the past studies using sulfuric acid, ammonia solution and nitric acid or $NH_3.H_2O$ (Asenciosa & Sun-Koub 2012; Amirsalari & Farjami Shayesteh 2015; Du *et al*, 2009).

The observation reported by(Amirsalari & Farjami Shayesteh 2015) confirms the best results were obtained in the slight alkaline value of 9and at a calcination temperature of 500°C. Diversities could be attributed to the different in resources, where the study was based on pure aluminum nitrate and not waste cans. Also, the precipitation was by adding ammonia solution whereas in the present study was hydrochloric acid. The retention of water present in aluminum hydroxide structure is strongly affected by the pH of precipitation step (Asenciosa & Sun-Koub 2012).The present results coincide with (Du *et al*, 2009) for they noticed that the formation of boehmite and amorphous aluminum oxide phases are favored during precipitation step in the acidic and neutral media with pH values increased from 5 to7 and switching to strong alkaline media (8-11) favored the formation of Bayerite (alpha alumina).

Effect of pH on Surface Area

As given in Table 5, the highest surface area of 311.14 m^2/g was obtained at pH 7.Further increase in pH to 12 is found to decrease the sample surface area to 275.23 m^2/g.

Table 5 Surface area of alumina synthesized at different pH values

pH	Surface Area(m^2/g)
3	279.11
7	311.14
12	275.23

The pH values during precipitation had a great influence on the surface area of alumina obtained, because it strongly affects the degree of aggregation and dissolution of alumina gel during aging (Asenciosa & Sun-Koub 2012). According to the present experimental results, gamma alumina with high surface area was acquired at neutral pH, while at acidic and basic conditions the dissolution of alumina grains led to produce alumina with lower surface area. The isoelectric point of $Al(OH)_3$ was found to be in pH range of 7-9 (Faust & Aly 1998). If the solution pH was less than the isoelectric point of $Al(OH)_3$, a positively charged aluminum hydroxides would be found. At higher pH values above the isoelectric point, then a negatively charged aluminum hydroxides would be existed (Du *et al*, 2009). The presence of positively and/or negatively charged aluminum hydroxide prevents aggregation and facilitates dissolution. For solution pH at isoelectric point, aggregation and precipitation will be predominated. This may explain the reason behind that maximum surface area of alumina obtained in the present study which was at aluminum hydroxide isoelectric point at pH 7.

The decrease in the surface area of this sample can be attributed to that some surface pores maybe blocked by very small crystals of alumina (Asenciosa & Sun-Koub 2012).Therefore, the sample at pH 7 and calcined at 550°C was subjected to AFM and XRF analysis. This result is in agreement with those obtained (Al-bayati *et al*, 2016), where gamma alumina catalyst were prepared from the digestion of α-Al_2O_3 with sodium hydroxide solution in autoclave to produce sodium aluminate which was precipitated at pH 6.5 as an optimum condition.

Atomic Force Microscopy (AFM)

To investigate the morphology of prepared alumina AFM test was utilized. Figures 7 and 8 showed topographical images on two and three-dimensional surface profile of alumina prepared at pH 7 and calcined at 550 ºC.

Table 6 Particle size distribution of synthesized alumina

Diameter(nm)<	Volume(%)	Cumulation(%)	Diameter(nm)<	Volume(%)	Cumulation(%)	Diameter(nm)<	Volume(%)	Cumulation(%)
45.00	1.77	1.77	65.00	13.27	37.17	85.00	11.50	94.69
50.00	5.31	7.08	70.00	15.93	53.10	90.00	5.31	100.00
55.00	4.42	11.50	75.00	13.27	66.37			
60.00	12.39	23.89	80.00	16.81	83.19			

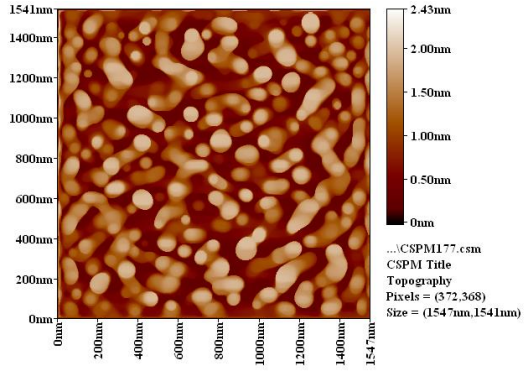

Fig 7 Two-dimensional image of the surface of synthesized alumina

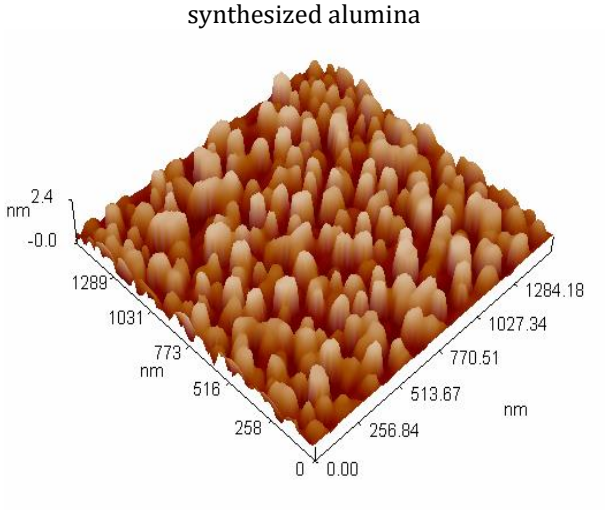

Fig 8 Three-dimensional image of the surface of synthesized alumina

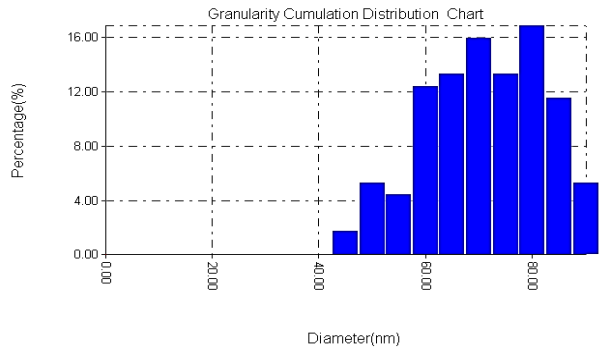

Fig 9 Granularity accumulation distribution report of synthesized alumina

Usually the range of nano particles is 1 – 100 nano meter (Tiwari & Tiwari 2014). Table 6 and figure 9 illustrate the particles size distribution of synthesized alumina. The results confirmed that the prepared alumina was in the nano size region for the range of the diameters was between 45 - 90 nm. Most volume percentage of particles was 16.81 % at size distribution of 80 nm, the lowest volume percentage was 1.77% for particles at size of 45 nm, and the average particle size was 68.56 nm.

X-Ray Fluorescence (XRF)

The purity of the prepared nano gamma alumina was confirmed by XRF analysis. The chemical composition of prepared sample is given in table 7. The prepared contains 79.46% Al_2O_3, 4.22% Na_2O, 4.18 % Cl , 1% SiO_2 and the balance of other components were as traces. The presence of NaCl salt in the alumina structure affected the crystallinity of this sample but did not affect the surface area. The pronounced encouraging results are promising for adopting the present study for future applications.

Table 7 Chemical composition of synthesized alumina

Symbol	Element	Wt%
Al_2O_3	Aluminum	79.46
Na_2O	Sodium	4.226
Cl	Chlorine	4.186
SiO_2	Silicon	1.000

Conclusion

The present study presents a facile method for recycling waste aluminum cans into a valuable nanoparticle gamma alumina catalyst with high degree of qualification for industrial applications. Investigations revealed that calcination at 550°C is convenient to produce high crystalline structure in spite of the increased crystallinity obtained at higher temperature considering the energy saving aspect. Also, the pH of precipitating aluminum oxide in the neutral region is an important factor and can produce high surface area of crystalline of 311m^2/g and nano size product of 68.56nm.

Acknowledgment

The authors are grateful to the Ministry of Oil in Iraq / Petroleum Research and Development Center for the financial support of the PhD degree project.

References

Al-bayati, A.D.J., Al-taee, H.A.M. & Faisal, I. (2016), Determination of the Optimum Conditions for the Production of Gamma Alumina (ɣ-Al_2O_3) By the Precipitation Method of the Sodium Aluminate Solution , *Journal of Engineering*, 17(2), pp79–86.

Al-rubaye, R. (2013), *Generation and Characterisation of Catalytic Films of Zeolite Y and ZSM-5 on FeCrAlloy Metal*: Ph.D. Thesis, University of Manchester.

Amirsalari, A. & Farjami Shayesteh, S. (2015), Effects of pH and calcination temperature on structural and optical properties of alumina nanoparticles, *Superlattices and Microstructures*, 82, pp 507–524.

An, B. *et al*. (2010), Azeotropic distillation-assisted preparation of nanoscale gamma-alumina powder from waste oil shale ash, *Chemical Engineering Journal*, 157(1), pp 67–72.

Asenciosa, Y.J.O. & Sun-Koub, M.R. (2012), Synthesis of high-surface-area gamma-Al_2O_3 from aluminum scrap and its use for the adsorption of metals : Pb (II), Cd (II) and Zn (II), *Optical Materials*, 34(9), pp 1553–1557.

Bell, T.E. *et al*. (2015), Single-step synthesis of nanostructured gamma-alumina with solvent reusability to maximise yield and morphological purity, *J. Mater. Chem. A*, 3, pp 6196–6201.

De Boer, J.H. & Lippens, B.C. (1964), Studies on pore systems in catalysts - II The two causes of reversible hysteresis, *Journal of Catalysis*, 3(1), pp 38–43.

Chen, Y.F. *et al*. (2003), The effect of calcination temperature on the crystallinity of TiO_2 nanopowders, *Journal of Crystal Growth*, 247(3–4), pp 363–370.

Chotisuwan, S. *et al*. (2012), Mesoporous alumina prepared from waste aluminum cans and used as catalytic support for toluene oxidation, *Materials Letters*, 70, pp125–127.

Das, B.R. *et al*. (2007), Production of η-alumina from waste aluminium dross, *Minerals Engineering*, 20, pp 252–258.

Dash, B. *et al*. (2008), Acid dissolution of alumina from waste aluminium dross, *Hydrometallurgy*, 92(1–2), pp 48–53.

Du, X. *et al*. (2009), Influences of pH value on the microstructure and phase transformation of aluminum hydroxide, *Powder Technology*, 192(1), pp 40–46.

Faust, S.D. & Aly, O.M. (1998), *Chemistry of Water Treatment, Second Edition*, CRC Press.

Fernando, J.A. & Chung, D.D.L. (2001), Improving an alumina fiber filter menbrane for hot gas filtration using an acid phosphate binder, *Journal of Naterial Science*, 36, pp 5079–5085.

Gaber, A. *et al*. (2014), Influence of calcination temperature on the structure and porosity of nanocrystalline SnO_2 synthesized by a conventional precipitation method, *International Journal of Electrochemical Science*, 9(1), pp 81–95.

Hosseini, S.A., Niaei, A. & Salari, D. (2011), Production of γ-Al_2O_3 from Kaolin, *Open Journal of Physical Chemistry*, 1(2), pp 23–27.

Hummadi, K.K. (2005), Influence of calcination temperature of Prepared Aluminum hydroxide on the activity of active gamma Alamina oxide on the dehydration of ethanol, *Eng. & Technology*, 24(4), pp 368–383.

Keshavarz, A.R., Rezaei, M. & Yaripour, F. (2010), Nanocrystalline gamma-alumina: A highly active catalyst for dimethyl ether synthesis, *Powder Technology*, 199(2), pp 176–179.

Liu, W. *et al*. (2011), Preparation of micron-sized alumina powders from aluminium beverage can by means of sol-gel process, *Micro and Nano Letters*, 6(10), pp 852–854.

Martínez, S.S. *et al*. (2007), Coupling a PEM fuel cell and the hydrogen generation from aluminum waste cans, *International Journal of Hydrogen Energy*, 32(15), pp3159–3162.

Matori, K.A. *et al*. (2012), Phase transformations of α-alumina made from waste aluminum via a precipitation technique, *International Journal of Molecular Sciences*, 13(12), pp 16812–16821.

Monshi, A., Foroughi, M.R. & Monshi, M.R. (2012), Modified Scherrer Equation to Estimate More Accurately Nano-Crystallite Size Using XRD, *World Journal of Nano Science and Engineering*, 2(3), pp 154–160.

Richardson, J.T. (1989), Principles of Catalysts Development.

Sheel, T.K. *et al*. (2016), Preparation of Aluminum Oxide from Industrial Waste Can Available in Bangladesh Environment: SEM and EDX Analysis, *Journal of Advanced Chemical Engineering*, 6(2).

Sickafus, K.E., Wills, J.M. & Grimes, N.W. (1999), Structure of spinel, *Journal of the American Ceramic Society*, 82(12), pp 3279–3292.

Sun, Z.X. *et al*. (2008), Effects of calcination temperature on the pore size and wall crystalline structure of mesoporous alumina, *Journal of Colloid and Interface Science*, 319(1), pp 247–251.

Taies, J.. & Mahmood, W.A. (2010), Preparation of activated alumina From Iraqi-kaoline clays for Catalysts support, *Baghdad Journal for Science*, 7(4), pp 1343–1348.

Tiwari, A. & Tiwari, A. (2014), *Bioengineered Nanomaterials*, CRC Press.

Wang, S. *et al*. (2008), Synthesis of γ-alumina via precipitation in ethanol, *Materials Letters*, 62(20), pp 3552–3554.

Yamaguchi, G., Yanagida, H. & Ono, S. (1964), A new alumina hydrate, "'tohdite'" (Al_2O_3_$5H_2O$), *Bull. Chem. Soc. Jpn.*, 37(5), pp 752–754.

Yaripour, F. *et al*. (2015), The effects of synthesis operation conditions on the properties of modified γ-alumina nanocatalysts in methanol dehydration to dimethyl ether using factorial experimental design, *Fuel*, 139, pp 40–50.

Zhang, Z. & Pinnavaia, T.J. (2008), Mesostructured Forms of the Transition Phases η- and χ-Al_2O_3, *Angewandte Chemie*, 120(39), pp 7611–7614.

Zou, H. *et al*. (2013), Hydrogen production by hydrolysis of aluminum, *Journal of Alloys and Compounds*, 578, pp 380–384.